analytical chemistry

pubs.acs.org/ac

Letter

Zero-Interfacing μHPLC to ICPMS

Yang Zhou, Xingrui Song, Xiaowen Yan, Limin Yang, Shi Chen, and Qiuquan Wang*

Cite This: *Anal. Chem.* 2022, 94, 16975−16979

Read Online

ACCESS | Metrics & More | Article Recommendations | Supporting Information

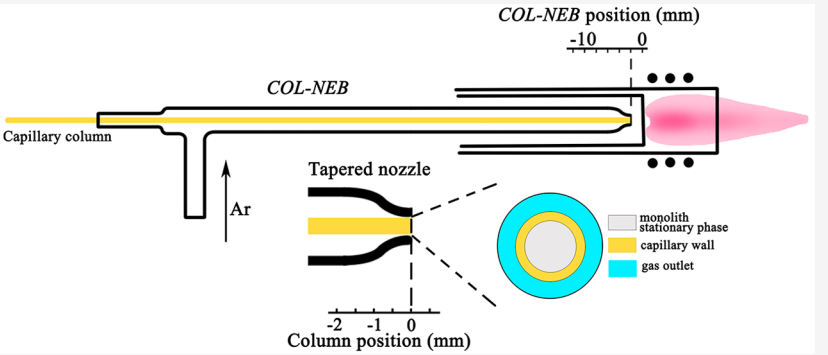

ABSTRACT: The chromatography−mass spectrometry hyphenated technique is the most widely adopted tool for quantifying trace analytes in a complex biosample. One issue we frequently encountered, however, is that the separated analyte-containing chromatographic peaks broaden and even remix prior to mass spectrometric quantification due to the inevitable molecular diffusion within the dead-volume introduced by hyphenation. We developed a zero-interfacing approach for coupling microbore (μ) HPLC with inductively coupled plasma mass spectrometry (ICPMS). Zero-interfacing μHPLC to ICPMS has been achieved by a column-nebulizer assembly (COL-NEB) of a self-designed glass framework with a tapered nozzle, in which a capillary chromatographic column can be harbored while an Ar gas flow is blown through the nozzle mouth. The COL-NEB can be positioned just before the base of the Ar-ICP serving as the central sampling channel of a conventional Ar-ICP torch for online nebulization and transportation of the analytes separated on μHPLC into ICPMS, maintaining the molecular resolution obtained on μHPLC and the limit of detection (LOD) of ICPMS. For example, the full width at half-maximum of a SLUGT peptide chromatographic peak was reduced to 1.71 ± 0.07 s (n = 5) with a 0.72 fg LOD (3σ) of ^{80}Se. Moreover, at least 32 Se-containing peptides were determined in the trypsin lysate of the water-soluble fraction (≥3000 MW) from Se-enriched yeast CRM SELM-1 within a 10 min run, the highest record to date. We believe such an approach paves the way to determining accurate information on a heteroatom and its binding biomolecules that play key roles during life processes.

Although mass spectrometry (MS) has been advancing into a real problem-solving tool with remarkable mass resolution to date, contributions from dynamic separation techniques such as sample preseparation and introduction units have been greatly valued. Coupling of microbore high-performance liquid chromatography (μHPLC) to MS is the most conventionally adopted method when encountering the problem of trace analytes in high abundance and a complex matrix that need to be analyzed. The online hyphenation between μHPLC and a soft-ionization MS, for example, electrospray ionization MS that generates intact gas-phase multivalent ions from the analytes in μHPLC effluent via analyte-dependent ionization mechanisms, is driven mainly by electric field and heat-desolvation.[1] In contrast, coupling of μHPLC with a hard ionization MS, typically Ar-based inductively coupled plasma quadrupole MS (ICPMS), was realized via the pneumatic nebulization of a droplet-composed aerosol from the effluent of μHPLC, followed by successive events from desolvation, vaporization, atomization, to ionization in Ar-ICP.[2] Such a process produces univalent-dominated atomic ions for further MS separation and measurement. During which, nebulization of the μHPLC effluent and aerodynamic extraction of the micrometer-sized fine droplets into Ar-ICP are vital for obtaining better analyte transportation and ionization efficiencies and thus a lower limit of detection (LOD) of the analytes on ICPMS. Input of the fine droplets into ICPMS was usually achieved via a spray chamber. However, the resulting sample introduction efficiency (SIE) was shown to be less than 5% in general,[3,4] although later developments of the cross-flow and microflow or nanoflow total consumption nebulizers with

Received: September 8, 2022
Accepted: November 4, 2022
Published: November 8, 2022

https://doi.org/10.1021/acs.analchem.2c03951
Anal. Chem. 2022, 94, 16975−16979

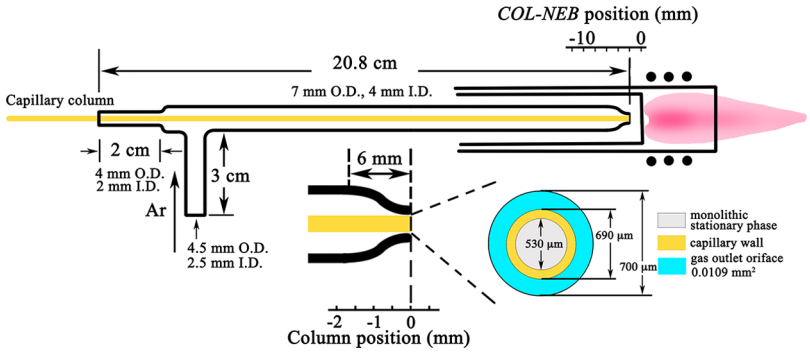

Figure 1. Schematic diagram of COL-NEB for zero-interfacing μHPLC to ICPMS. The glass framework together with a capillary chromatographic column from COL-NEB, in which the position of the capillary monolithic column outlet end related to the nozzle mouth of the glass framework and that of COL-NEB to the base of Ar-ICP can be adjusted. Moreover, the nozzle mouth I.D. can also be accordingly designed and fabricated depending on the O.D. of the chromatographic column used.

spray chambers of a few cubic centimeters significantly improved the SIE.[5−7] It should be noted that despite the small volume of the spray chamber used, it did enlarge the dead-volume between the μHPLC and ICPMS, causing the risk that the individual chromatographic peaks undergo peak-broadening and even that chromatography-separated analytes remix prior to ICPMS. This is because the inevitable chemical concentration-driven isotropic molecular diffusion is always present. Particularly critical to ICPMS, an element/isotope-specific mass detector measures the amounts of the atomic isotope ions generated indiscriminately from almost all molecules, since not only the total amount of the element in a sample but also information on which molecule the element bonds to or is incorporated within are desired.[8] A direct-injection high efficiency nebulizer (DIHEN) without using a spray chamber[9−11] that was derived from the combination of a direct injection nebulizer (DIN)[12,13] and a high-efficiency nebulizer (HEN)[14,15] was a successful example among the previously reported nebulizers for micro amounts of sample introduction into ICPMS. Nevertheless, even when DIHEN and/or DIN were used as the interface between μHPLC and ICPMS, a transport capillary must be used for connecting the chromatographic column and delivering and nebulizing the chromatographic effluent into ICPMS. The dead-volume from a few to dozens of microliters introduced by the transport capillary does matter, because the molecular diffusion is equal along all directions, and more importantly, the diffusion kinetics is much faster in a pure liquid medium within the transport capillary in comparison to that in a solid−liquid medium containing a stationary phase and mobile phase in the chromatographic column. The faster "horizontal direction" molecular diffusion along the centimeters long transport capillary (even though its inner diameter was micrometers wide) should be definitely responsible for the resulting peak-width of dozens of seconds or even minutes demonstrated in previous reports. Such a duration of seconds to minutes certainly broadens the chromatographic peaks and possibly causes re-overlapping of the just baseline-separated analytes on μHPLC, suppressing the chromatographic peak capacity and thus losing important information regarding which molecule the element bonds to or is incorporated within. We hypothesize that such a duration time would be eliminated if the corresponding dead-volume that accompanies the coupling of μHPLC with ICPMS could be removed.

Herein, we report a zero-interfacing approach for coupling μHPLC with ICPMS. A self-designed glass framework with a ventilation branch and a gradually tapered nozzle (Figures 1 and S1) was designed and fabricated, in which a capillary chromatographic column can be centrally harbored while Ar gas can be blown through for gas−liquid interaction and thus the nebulization of the μHPLC effluent. The glass framework together with the capillary chromatographic column assemble into a column-nebulizer (COL-NEB). Such a COL-NEB serves as the central sampling channel of the Ar-ICP torch and can be flexibly inserted into the base of the Ar-ICP. It allows the zero-interfacing between μHPLC and ICPMS, eliminating the dead-volume resulting from the transport capillary used in DIN and DIHEN and thus maintaining the sound molecular resolution obtained on μHPLC prior to ICPMS. To demonstrate this proposal, a homemade 690 μm O.D. × 530 μm I.D. methacrylated-C18 hybrid silica-fused capillary monolithic column[16] was used to separate Se-containing peptides on μHPLC and measured by ICPMS.

As mentioned above, nebulization of the micrometer-sized droplets from the effluent of μHPLC into Ar-ICP is an essential factor for achieving an efficient ICPMS quantification. We know that nebulization is accomplished by the interaction between gas and liquid. Adequate gas−liquid interaction leads to smaller droplet size that benefits not only a high sample introduction but also an efficient ionization. Droplet size is usually expressed in terms of the Sauter mean diameter (D_{32}/d_c) that can be defined by the following semiempirical formula:[17]

$$\frac{D_{32}}{d_c} = C_1\left[\frac{\Delta P_g^*}{(1+\mu)^2}\right]^m (1 + C_2 On^j) \quad (1)$$

where C_1, C_2, m, and j are all constants determined by nebulizer design ($m < 0$). On is the Ohnesorge number [$On = \frac{\eta_l}{\sqrt{\rho_l \sigma_l L_l}}$, in which η_l is the liquid viscosity (here 3.0×10^{-3} Pa·s for H_2O and 0.29×10^{-3} ACN); ρ_l is the liquid density (1.0 g/cm^3 for H_2O and 0.79 ACN); σ_l is the surface tension of liquid (72.75 dyn/cm for H_2O and 26.58 ACN); and L_l is the characteristic length of liquid that is equal to the liquid outlet diameter of the capillary, d_c.]. This formula means that D_{32}/d_c is dominated by the nebulizer geometry, gas pressure difference ΔP_g*, and the liquid-to-gas mass flow ratio $\mu = m_l/m_g$. When Ar is used as the nebulization gas, which is consistent with ICPMS plasma gas, and the homemade capillary monolithic column with appropriate mobile phase composition and flow rate is used for μHPLC, significant factors that affect the nebulization performance are the flow rate of Ar nebulization gas and the structure of the COL-NEB. We thus adjusted the column outlet end relative

https://doi.org/10.1021/acs.analchem.2c03951
Anal. Chem. 2022, 94, 16975−16979

to the nozzle mouth from retracted from (−2.0 mm), flush with (0.0), to protruded outside (0.5 mm) the nozzle mouth with 0.5 mm stepwise manner.[2] Such assembled COL-NEBs were inserted just before the base of the Ar-ICP replacing the central sampling channel of the Ar-ICP torch. The experimental results shown in Figure S2A indicate that the ICPMS signal intensities of both ^{115}In measured under standard mode and ^{80}Se under CH_4 DRC at the ratio of CeO/Ce ≤ 0.025 (Table S1) increased along with the increase in ΔP_g* from 1.02 psi at −2.0 mm to 52.07 psi at 0.0 mm when the sample solution and nebulization Ar gas flow rates were set at 50 μL/min and 0.5 L/min. The maximum signal intensities of ^{115}In 57481 ± 866 cps (n = 5) and ^{80}Se 21160 ± 877 cps (n = 5) of 1 μg/L each were obtained when the outlet end of the column was flush with the nozzle mouth; even though the ΔP_g* was a little bit higher (58.27 psi) at 0.5 mm protruded outside the nozzle mouth, the signal dropped to ^{115}In 21294 ± 1032 cps and ^{80}Se 7704 ± 142 cps (n = 5). The reason for this phenomenon might be attributed to the thick wall (80 μm) of the capillary monolithic column used, which causes the nebulizer gas to be partly shielded and not fully interacting with the μHPLC effluent, resulting in less nebulization and thus the lower signal intensity. Therefore, the column flush with the nozzle mouth was selected and used throughout this study. In this case, the orifice area formed between the capillary column and the nozzle mouth for the gas−liquid interaction is the smallest (0.0109 mm^2) with the ΔP_g* of 52.07 psi. Regarding the relative position of the COL-NEB to the base of Ar-ICP, the closer the COL-NEB, the higher the ICPMS intensities achieved because more generated droplets can be transported into the ICPMS. As expected, the experimental results obtained indicated that the ICPMS signal intensities of both ^{115}In and ^{80}Se increased with approaching COL-NEB to the base of Ar-ICP (Figure S2B). It should be noted that the intensity of ^{115}In 56327 ± 754 cps (n = 5) at 0.0 cm position of COL-NEB relative to the base of Ar-ICP is just a little bit higher than the 55399 ± 721 cps (n = 5) at −0.2 cm. The same is true for ^{80}Se, 20032 ± 806 cps (n = 5) at 0.0 cm and 19536 ± 346 cps (n = 5) at −0.2 cm, meaning similar droplet transportation efficiency. We thus positioned COL-NEB at −0.2 cm from the base ofthe Ar-ICP just in case of possible damage, although it can be located at 0.0 cm because the temperature at the base of Ar-ICP is only about 90 °C, which is safe enough for any capillary column. Subsequently, the influence of the nebulization Ar gas flow rate on the ICPMS signal intensity of ^{115}In and ^{80}Se was investigated at the sampling flow rate of 50 μL/min. The obtained results indicated that their ICPMS signal intensity increased first and then decreased along with the increase from 0.4 to 0.8 L Ar/min (Figure S2C). No matter for ^{115}In or ^{80}Se, the highest intensity was observed at 0.54 L/min, 56334 ± 497 cps ^{115}In and 19074 ± 128 cps ^{80}Se (n = 5). The increasing ICPMS intensity along with the increase in the nebulization Ar gas flow rate from 0.4 to 0.54 L/min can be attributed to the decrease in liquid−gas mass flow ratio μ from 0.070 to 0.052 and the increase in ΔP_g* from 39.04 to 57.02 psi according to the semiempirical formula 1; an Ar gas flow rate higher than 0.54 L/min causes the droplets to have not only a shorter stay in the Ar-ICP for ionization but also more dilutive dispersion besides the insignificant cooling effect on the temperature of Ar-ICP, leading to lower ionization efficiency, fewer ions entering into the sampler cone, and thus a lower ICPMS signal intensity.[18]

The primary motivation of this study is to zero-interface μHPLC to ICPMS for retaining the chromatographic resolution gained on μHPLC prior to ICPMS measurement. After optimization of the COL-NEB working conditions, we compared the performance of COL-NEB with the commercially available Meinhard concentric nebulizer TRP-50-C0 and micronebulizer HEN working with a 15 mL cyclonic spray chamber as well as a self-made DIN of 67 μL dead-volume mimetic to DIHEN as the interface,[10,11] regarding the full width at half-maximum (FWHM) of the chromatographic peak. The Se-pentapeptide SLUGT was tested on the 30 cm long methacrylated-C18 monolithic capillary column with a 10 min gradient elution of 5% to 95% ACN containing 0.05% TFA. It was clear that TRP-50-C0 and HEN with the same cyclonic spray chamber are not good for interfacing μHPLC and ICPMS, because both the fwhm of 11.13 ± 0.41 s (n = 5) of the SLUGT chromatographic peak using TRP-50-C0 with the maximum ICPMS signal intensity of 9693 ± 194 cps (n = 5) and 15.39 ± 0.44 s (n = 5) with 170218 ± 3356 cps (n = 5) HEN shown in Figure 2 are too large because of the 15 mL large cyclonic spray

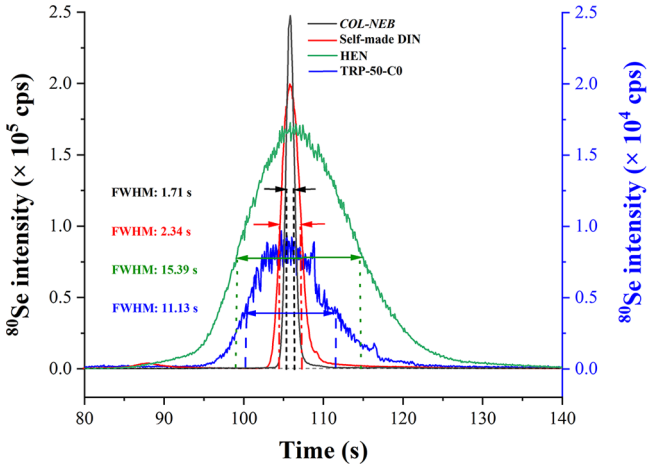

Figure 2. Interface-dependent FWHM of SLUGT chromatographic peak. Blue peak: TRP-50-C0 together with a 15 mL cyclonic spray chamber with the sheath flow of 2% HNO_3 at 0.3 mL/min. Green peak: HEN without the sheath flow but with the same 15 mL spray chamber. Red peak: the self-made DIN. Black peak: COL-NEB. The sample volume for each run was 500 nL of 1.0 μmol/L SLUGT. Detailed experimental procedures and instrumental operating conditions are described in the Supporting Information and listed in Table S1.

chamber dead-volume involved. The FWHM shortened to 2.34 ± 0.12 s (n = 5) with the ICPMS signal intensity of 196587 ± 3598 cps (n = 5) using the self-made DIN. By comparison, when using the COL-NEB zero-interface to couple μHPLC and ICPMS, the FWHM reduced further to 1.71 ± 0.07 s (n = 5) with 247660 ± 4161 cps (n = 5). Evidently, COL-NEB is the best interface for coupling μHPLC and ICPMS considering the narrowest fwhm and highest ICPMS signal intensity obtained. This is due to elimination of the dead-volume raised from the "additional" transport capillary, resulting in the negligible time for the inevitable chemical concentration-driving isotropic molecular diffusion prior to ICPMS. Under the optimum conditions, on the other hand, the LOD (3σ) of Se as exemplified here reaches 1.8 × 10^{-5} nmol/L (1.44 ng/L), corresponding to an absolute 0.72 fg when monitoring ^{80}Se. Such a lower LOD achieved does benefit from the COL-NEB zero-interface developed. Yet involvement of the monolithic

https://doi.org/10.1021/acs.analchem.2c03951
Anal. Chem. 2022, 94, 16975−16979

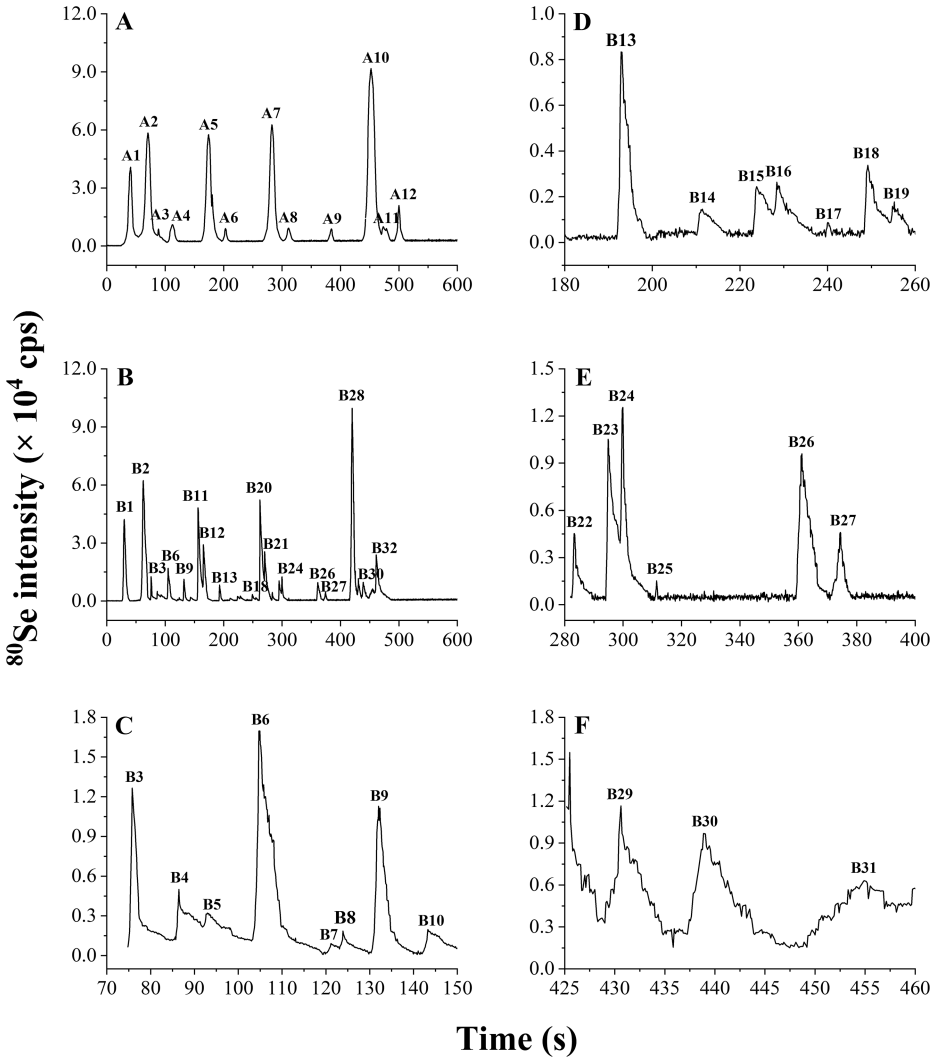

Figure 3. Quantification of Se-peptides in the trypsin lysate of the water-soluble fraction (≥3000 MW) from Se-enriched yeast CRM SELM-1. The chromatogram obtained using the self-made DIN interfaced μHPLC-ICPMS (A) and those using μHPLC-(COL-NEB)-ICPMS (B−F). Detailed sample pretreatment procedures and instrumental operating conditions are described in the Supporting Information and listed in Table S1.

stationary phase with 1.8 μm mean through-pore size[16] in the capillary column that provides multiple micrometer paths available for the chromatographic effluent prior to nebulization should not be overlooked, which contributed to the fine droplet generation. Moreover, the ICPMS ^{80}Se signal intensities of SLUGT kept stable with the RSDs of 4.6% for peak area [$(1.33 \pm 0.07) \times 10^6$, $n = 5$] and 1.2% retention time (106.80 ± 1.31 s, $n = 5$) (Figure S3), and no obvious carbon deposit over the ICPMS sampler cone was observed after running for over 24 h.

In order to demonstrate the efficacy of the COL-NEB-interfaced μHPLC-ICPMS [μHPLC-(COL-NEB)-ICPMS], we first extracted the water-soluble fraction from the selenium-enriched yeast CRM SELM-1, then ultrafiltered the sample using a hyperfiltration tube of 3000 MW to obtain the molecular weight greater than 3000 MW fraction. The fraction was subjected to trypsin digestion (for details, see the Supporting Information). The total Se content in the trypsin lysate was directly determined using ICPMS to be 270.37 ± 2.34 μg/L ($n = 5$); in parallel, the Se-containing peptides in the trypsin lysate were analyzed using μHPLC-(COL-NEB)-ICPMS. The obtained results indicated that at least 32 Se-peptides were quantified (Figure 3B−F); while at most 12 Se-peptides were determined when using the self-made DIN to interface μHPLC to ICPMS (Figure 3A). In addition, the individual Se-peptides were quantified without and with the addition of 5% O_2 into Ar-ICP according to their peak areas in the calibration curve (Figure S4) and normalized separately by the response factors relative to that of SLUGT (21% ACN) under different ACN% from 5 to 57% in the chromatographic elution gradient at the individual peak's retention time (Tables S2 and S3). The summed amount of Se in the 32 Se-peptides was calculated to be 249.03 ± 3.41 μg/L ($n = 5$) (without O_2) and 250.13 ± 3.41 μg/L ($n = 5$) (with O_2), corresponding to the recoveries of Se (92.1 ± 1.3)% and (92.5 ± 1.3)% ($n = 5$) relative to the amount of total Se. It should be noted that the recoveries obtained with and without the addition of O_2 are similar. This might be due to the content of ACN at the retention time of SLUGT (106.80 ± 1.31 s, $n = 5$) around the middle of the elution gradient compromising the C-effect, although the Se ICPMS response factors increase along with the increase in ACN% in the gradient (Figures S5 and S6). The discrepancy between the total amount of Se directly determined using ICPMS and the sum of Se quantified using μHPLC-(COL-NEB)-ICPMS might be more accurately corrected using isotope dilution or the addition of C-containing

https://doi.org/10.1021/acs.analchem.2c03951
Anal. Chem. 2022, 94, 16975−16979

gas to the plasma in the future.[19,20] Regardless, COL-NEB does improve the analytical performance of μHPLC-ICPMS in providing richer information on possible Se existing chemical forms in the CRM SELM-1 rather than the total Se content. Such richer information on Se-peptides, on the other hand, poses challenges for further identification using soft-ionization molecular MS.

In conclusion, for the first time COL-NEB optimally achieved zero-interfacing μHPLC to ICPMS featuring the most Se-containing peptides quantified in the trypsin lysate of the CRM SELM-1 and lowest detection limit achieved to date. We believe that such a zero-interfacing design may be applied to other situations, not limited to Se-species and the monolithic C18 capillary column-based reversed phase μHPLC demonstrated here, considering the complexity of a biological sample needs different separation mechanism-based μHPLC coupled with ICPMS for separating and quantifying different targeted analytes. More detailed information regarding which molecule the element bonds to or is incorporated within will be discovered once the corresponding molecule standards are available. In addition, we believe the combined use of the structure-specific soft-ionization MS together with μHPLC-(COL-NEB)-ICPMS will offer more information on both the heteroatom and its bonding biomolecules that need to be elicited, deepening our understanding of life sciences.

■ ASSOCIATED CONTENT

Supporting Information

The Supporting Information is available free of charge at https://pubs.acs.org/doi/10.1021/acs.analchem.2c03951.

> Reagents and materials, design and fabrication of COL-NEB, pretreatment of CRM SELM-1, and Se-containing peptides analysis; photographs of the COL-NEB interface and the nozzle, optimization of experimental conditions, and calibration (Figures S1−S6); operation conditions of μHPLC-ICPMS and results of Se-peptide quantification in CRM SELM-1 (Tables S1−S3) (PDF)

■ AUTHOR INFORMATION

Corresponding Author

Qiuquan Wang − *Department of Chemistry & the MOE Key Laboratory of Spectrochemical Analysis and Instrumentation, College of Chemistry and Chemical Engineering, Xiamen University, Xiamen 361005, China;* orcid.org/0000-0002-5166-4048; Email: qqwang@xmu.edu.cn; Fax: +86 592 2187400

Authors

Yang Zhou − *Department of Chemistry & the MOE Key Laboratory of Spectrochemical Analysis and Instrumentation, College of Chemistry and Chemical Engineering, Xiamen University, Xiamen 361005, China*

Xingrui Song − *Department of Chemistry & the MOE Key Laboratory of Spectrochemical Analysis and Instrumentation, College of Chemistry and Chemical Engineering, Xiamen University, Xiamen 361005, China*

Xiaowen Yan − *Department of Chemistry & the MOE Key Laboratory of Spectrochemical Analysis and Instrumentation, College of Chemistry and Chemical Engineering, Xiamen University, Xiamen 361005, China;* orcid.org/0000-0001-6608-6044

Limin Yang − *Department of Chemistry & the MOE Key Laboratory of Spectrochemical Analysis and Instrumentation, College of Chemistry and Chemical Engineering, Xiamen University, Xiamen 361005, China*

Shi Chen − *Department of Chemistry & the MOE Key Laboratory of Spectrochemical Analysis and Instrumentation, College of Chemistry and Chemical Engineering, Xiamen University, Xiamen 361005, China*

Complete contact information is available at: https://pubs.acs.org/10.1021/acs.analchem.2c03951

Notes

The authors declare no competing financial interest.

■ ACKNOWLEDGMENTS

This study was financially supported by the National Natural Science Foundation of China (22193053, 21874112, and 21535007).

■ REFERENCES

(1) Konermann, L.; Ahadi, E.; Rodriguez, A. D.; Vahidi, S. *Anal. Chem.* **2013**, *85*, 2−9.

(2) Beauchemin, D., Ed.; *Sample Introduction Systems in ICPMS and ICPOES*; Elsevier: Amsterdam, 2020.

(3) Sharp, B. L. *J. Anal. At. Spectrom.* **1988**, *3*, 939−963.

(4) Mora, J.; Maestre, S.; Hernandis, V.; Todolí, J. L. *TrAC Trends in Analytical Chemistry* **2003**, *22*, 123−132.

(5) Li, J.; Umemura, T.; Odake, T.; Tsunoda, K. *Anal. Chem.* **2001**, *73*, 1416−1424.

(6) Schaumloffel, D.; Encinar, J. R.; Lobinski, R. *Anal. Chem.* **2003**, *75*, 6837−6842.

(7) Giusti, P.; Lobinski, R.; Szpunar, J.; Schaumlöffel, D. *Anal. Chem.* **2006**, *78*, 965−971.

(8) Clough, R.; Harrington, C. F.; Hill, S. J.; Madrid, Y.; Tyson, J. F. *J. Anal. At. Spectrom.* **2021**, *36*, 1326−1373.

(9) McLean, J. A.; Zhang, H.; Montaser, A. *Anal. Chem.* **1998**, *70*, 1012−1020.

(10) Acon, B. W.; McLean, J. A.; Montaser, A. *J. Anal. At. Spectrom.* **2001**, *16*, 852−857.

(11) Wind, M.; Eisenmenger, A.; Lehmann, W. D. *J. Anal. At. Spectrom.* **2002**, *17*, 21−26.

(12) Lawrence, K. E.; Rice, G. W.; Fassel, V. A. *Anal. Chem.* **1984**, *56*, 289−292.

(13) Shum, S. C. K.; Pang, H.; Houk, R. S. *Anal. Chem.* **1992**, *64*, 2444−2450.

(14) Nam, S. H.; Lim, J. S.; Montaser, A. *J. Anal. At. Spectrom.* **1994**, *9*, 1357−1362.

(15) Pergantis, S. A.; Heithmar, E. M.; Hinners, T. A. *Anal. Chem.* **1995**, *67*, 4530−4535.

(16) Xu, Z. D.; Yang, L. M.; Wang, Q. Q. *J. Chromatogr. A* **2009**, *1216*, 3098−3106.

(17) Groom, S.; Schaldach, G.; Ulmer, M.; Walzel, P.; Berndt, H. *J. Anal. At. Spectrom.* **2005**, *20*, 169−175.

(18) Zhou, Y.; Chen, Z. Q.; Zeng, J. X.; Zhang, J. X.; Yu, D. X.; Zhang, B.; Yang, L. M.; Yan, X. W.; Wang, Q. Q. *Anal. Chem.* **2020**, *92*, 5286−5293.

(19) Calderon-Celis, F.; Cid-Barrio, L.; Encinar, J. R.; Sanz-Medel, A.; Calvete, J. J. *J. Proteomics* **2017**, *164*, 33−42.

(20) Calderon-Celis, F.; Sanz-Medel, A.; Encinar, J. R. *Chem. Commun.* **2018**, *54*, 904−907.